Draft version October 7, 2002
Preprint typeset using LaTeX style emulateapj v. 19/02/01

GRAVITATIONAL WAVES FROM RELATIVISTIC ROTATIONAL CORE COLLAPSE

Harald Dimmelmeier[1], José A. Font[2] and Ewald Müller[3]
Max-Planck-Institut für Astrophysik, Karl-Schwarzschild-Str. 1, D-85740 Garching, Germany.
Draft version October 7, 2002

ABSTRACT

We present results from simulations of axisymmetric relativistic rotational core collapse. The general relativistic hydrodynamic equations are formulated in flux-conservative form and solved using a high-resolution shock-capturing scheme. The Einstein equations are solved assuming a conformally flat 3-metric and the quadrupole formula is used to extract waveforms of the gravitational radiation emitted during the collapse. A comparison of our results with those of Newtonian simulations shows that the wave amplitudes agree within 30%. Surprisingly, in some cases, relativistic effects actually diminish the amplitude of the gravitational wave signal. We further find that the parameter range of models suffering multiple coherent bounces due to centrifugal forces is considerably smaller than in Newtonian simulations.

Subject headings: supernovae: general — hydrodynamics — relativity — gravitational waves

For more than two decades astrophysicists struggle to compute the gravitational wave signal produced by rotational core collapse supernovae (see e.g. Müller (1998)). Besides the coalescence of compact black hole or neutron star binaries, these events are considered as one of the most promising (burst) sources to detect gravitational waves (Thorne 1997). Theoretical predictions are still hampered by two major reasons: Firstly, the rotational state of the core prior to its gravitational collapse is not known, as multi-dimensional evolutionary calculations of rotating stars have not yet been performed. Up to now only quasi-spherical stellar pre-collapse models with a phenomenological description of mixing and angular momentum transport are available (Heger et al. 2000). Thus, predictions from rotational core collapse must rely upon extensive parameter studies. Secondly, reliable collapse simulations require a relativistic treatment of the dynamics, as both high densities and velocities together with strong gravitational fields are encountered, as well as the incorporation of a realistic equation of state (EoS) and neutrino transport. All previous studies have either neglected or approximated one or all of these requirements. In addition, most simulations assumed axisymmetry, the fully three-dimensional case still remaining essentially unexplored.

Concerning the gravitational wave signal the two most advanced studies of axisymmetric rotational core collapse to date have either investigated a few Newtonian models with a realistic EoS and simplified neutrino treatment (Mönchmeyer et al. 1991), or a large set of Newtonian models with a simplified EoS and no neutrino transport (Zwerger & Müller 1997). These simulations predict that nonspherical core collapse supernovae emit at most $\sim 10^{-6} M_\odot c^2$ in the form of gravitational radiation ($M_\odot = 1.99 \times 10^{33}$ g is the solar mass, and c is the speed of light). Thus, the collapse dynamics is not influenced by the gravitational radiation backreaction. The corresponding maximum quadrupole wave amplitude is $A_{20}^{\rm E2} \sim 10^3$ cm. For a source at a distance R this yields a maximum dimensionless strain $h \sim 10^{-23} \cdot (10\ {\rm Mpc}/R)$. Similar signal strengths have been found in non-axisymmetric Newtonian simulations using a simplified EoS and neglecting neutrino transport (Rampp et al. 1998).

The present work is a further step to improve the reliability of the prediction of the gravitational wave signal from rotational core collapse. To this end we have performed the first study (to our knowledge) in the relativistic framework, extending the axisymmetric Newtonian core collapse simulations of Zwerger & Müller (1997).

In order to be able examine a large set of collapse conditions we approximate the collapsing core by a rotating polytrope and use a simplified analytic EoS (Janka et al. 1993). We neglect all transport effects but include relativistic dynamics in a time-dependent spacetime. The pressure P consists of a polytropic part $P_{\rm p}$ and a thermal part $P_{\rm th}$,

$$P(\rho, \epsilon) = P_{\rm p} + P_{\rm th} = K \rho^{\gamma_{\rm p}} + \rho \epsilon_{\rm th} (\gamma_{\rm th} - 1), \qquad (1)$$

where ρ is the rest-mass density, and $\epsilon = \epsilon_{\rm p} + \epsilon_{\rm th}$ is the specific internal energy which consists of a polytropic and a thermal contribution. The polytropic constant K and the polytropic index $\gamma_{\rm p}$ change discontinuously at nuclear matter density, $\rho_{\rm nuc} = 2.0 \times 10^{14}$ g cm^{-3}, but are assumed to be independent of ρ elsewhere. The quantity $P_{\rm th}$ mimics the thermal pressure in the matter heated up by the shock. Writing P as a sum of these two terms prevents matter elements from following the same P–ρ-history during infall and expansion after bounce (for more details see Janka et al. (1993)). In all models we set $\gamma_{\rm th} = 1.5$, which corresponds to a mixture of relativistic and nonrelativistic gas.

The initial configurations are rotating relativistic stellar cores in equilibrium computed by means of Hachisu's self-consistent field method (Komatsu et al. 1989). All initial models are 4/3-polytropes, $P = K \rho^{4/3}$, with a central density of 1.0×10^{10} g cm^{-3}. They rotate according to the differential rotation law specified in Komatsu et

[1] harrydee@mpa-garching.mpg.de.
[2] font@mpa-garching.mpg.de.
[3] ewald@mpa-garching.mpg.de.

al. (1989), in which a parameter A (a length scale) determines the angular momentum distribution. For large values of A (compared to the size of the initial model) the configurations rotate almost rigidly, while small values of A correspond to strongly differentially rotating ones. This rotation law is the relativistic extension of the Newtonian one in Eriguchi & Müller (1984). The second parameter of the initial model is the ratio of the rotational energy to the modulus of the gravitational potential energy, $\beta = E_{\rm rot}/|E_{\rm pot}|$. The collapse is initiated by suddenly reducing $\gamma_{\rm p}$ from its initial value 4/3 to some prescribed value in the range $[1.28, 1.325]$. In all simulations we assume both axial and equatorial plane symmetry, and do not consider any physical angular momentum transport.

The hydrodynamic evolution of a relativistic fluid in an arbitrary spacetime endowed with a metric $g_{\mu\nu}$ is governed by the local conservation laws of the current density $J^\mu = \rho u^\mu$ and the (perfect fluid) stress-energy $T^{\mu\nu} = \rho h u^\mu u^\nu + P g^{\mu\nu}$, where u^μ is the 4-velocity and $h = 1 + \epsilon + P/\rho$ is the specific enthalpy. To derive the hydrodynamic equations, we introduce a set of conserved variables $D = \rho W$ (rest-mass density), $S_i = \rho h W^2 v_i$ (momentum density) and $E = \rho h W^2 - P$ (total energy density), $W = \alpha u^0$ being the relativistic Lorentz factor, in terms of the primitive variables (ρ, v_i, ϵ), where v_i is the 3-velocity. The resulting equations can be written as a first-order flux-conservative hyperbolic system of conservation laws (Banyuls et al. 1997).

The time-dependent metric is evolved using the $3+1$ splitting of spacetime. In this formalism the Einstein equations are written as a system of evolution and constraint equations for the 3-metric γ_{ij} and the extrinsic curvature K_{ij} (Arnowitt–Deser–Misner (ADM) equations). Unfortunately, achieving long-term stable evolution using the $3+1$ system (or improved reformulations) is still an open issue, although recently some progress has been accomplished (see Alcubierre et al. (2000) and references therein). Therefore, following Wilson et al. (1996)[4], we approximate the spacetime geometry by assuming that the 3-metric is conformally flat, i.e., $\gamma_{ij} = \phi^4 \hat{\gamma}_{ij}$ where ϕ is a conformal factor depending on the coordinates x^μ, and where $\hat{\gamma}_{ij}$ is the flat 3-metric (conformal flatness condition – CFC). In this approximation, the Einstein equations transform into a system of 5 coupled nonlinear elliptic equations for the conformal factor ϕ, the lapse function α and the shift vector β^i:

$$\hat{\Delta}\phi = -2\pi\phi^5(\rho h W^2 - P) - \tfrac{1}{8}\phi^5 K_{ij}K^{ij}, \qquad (2)$$

$$\hat{\Delta}(\alpha\phi) = 2\pi\alpha\phi^5(\rho h(3W^2 - 2) + 5P) + \tfrac{7}{8}\alpha\phi^5 K_{ij}K^{ij}, \qquad (3)$$

$$\hat{\Delta}\beta^i = 16\pi\alpha\phi^4 S^i + 2K^{ij}\hat{\nabla}_j\left(\frac{\alpha}{\phi^6}\right) - \tfrac{1}{3}\hat{\nabla}^i\hat{\nabla}_k\beta^k, \qquad (4)$$

with $\hat{\Delta}$ and $\hat{\nabla}$ being the flat space Laplace and Nabla operators, respectively.

The above approximation is exact in spherical symmetry, and makes no explicit assumptions on whether the evolution is stationary or dynamic. The CFC metric equations for the conformal factor ϕ (2) and the shift vector β^i (4) are identical to the ADM constraints, while the equation for the lapse function α (3) is derived from the maximal slicing condition and the trace of the ADM evolution equations for K_{ij}. The CFC provides an adequate approximation for investigations of rotational core collapse (beyond the Newtonian limit), as (i) the cores do not deviate much from spherical symmetry (contrary to binary neutron star mergers (Wilson et al. 1996)), and as (ii) gravitational radiation reaction is negligible for the dynamics.

The accuracy of the CFC approach has been considered by Cook et al. (1996), who find remarkably good results for rapidly rotating relativistic stars in equilibrium, with typical errors for different variables smaller than 5%. The accuracy degrades for extremely relativistic nonspherical configurations, e.g., rigidly rotating infinitesimally thin disks of dust (Kley & Schäfer 1999). Tests performed by us show that for rapidly rotating equilibrium configurations, the CFC metric approximates the exact ADM metric very well even for relativistic and strongly deformed spacetimes. They further show that the CFC equivalent of the ADM evolution equation for γ_{ij} is solved to high accuracy, while the ADM evolution equation for some components of K_{ij} is violated for nonspherical configurations. However, this equation need not be solved in the CFC approach as the metric components ϕ, α, and β^i are determined by the independent equations (2–4). The violations in the ADM equation for K_{ij} have no influence on the ability of the CFC metric to approximate the exact metric accurately, even in the case of highly relativistic rotating neutron stars. A direct comparison of our results with fully relativistic ADM simulations will be presented elsewhere.

As the off-diagonal elements of γ_{ij} are set to zero in the CFC approach, the gravitational wave content of the spacetime (the transverse part of the metric tensor) is eliminated. Therefore, to compute the gravitational wave signal we use the Einstein quadrupole formula in a post-processing step.

In order to exploit the hyperbolic and conservative character of the hydrodynamic equations, we have implemented in our code a Godunov-type flux-conservative finite volume scheme based on the solution of approximate Riemann problems at each cell interface (see, e.g. Font (2000)). On each time slice, the hydrodynamic data are represented by cell averages of the conserved quantities D, S_i and E. These are propagated to the next time level by a conservative Runge–Kutta algorithm, which involves the numerical fluxes and sources. The metric equations (2–4) are discretized on a 2-dimensional grid with a 9-point stencil. A Newton–Raphson iteration scheme is used to obtain the solution for the 5 metric functions. In each iteration, we have to solve a linear system of equations involving the (sparse) Jacobian matrix of the discretized equations.

We have performed a comprehensive number of tests of our code. Firstly, we have studied its ability to keep rotating neutron stars in equilibrium. To that end we have solved the relativistic hydrostatic equilibrium equations for rotating axisymmetric polytropes having different central densities, angular momentum profiles, and rotation velocities up to the mass-shedding limit. These initial data were evolved both on a static background metric and in a fully dynamic spacetime, always finding stability of the equilibrium configurations over many rotation periods. Secondly, we have compared the performance of our Eulerian code with a May–White-type Lagrangian artificial

[4] See Flanagan (1999); Mathews & Wilson (2000) for corrections.

viscosity code (May & White 1966) in spherical symmetry. When evolving identical collapse models with both codes we observe agreement in the evolution of fluid and metric variables within a few percent.

In order to pin down the effects of general relativity on rotational core collapse, we have compared relativistic (R) and Newtonian (N) simulations for a large set of initial models. The simulations have been performed in spherical coordinates using a logarithmic radial grid with 200 zones and an equidistant angular grid with 30 zones. Test runs with finer grids yield similar results. During a typical relativistic simulation the metric is calculated every 100th (10th) time step for a central density smaller (higher) than $0.1\rho_{\rm nuc}$, and extrapolated in between. A comparison with a run where the metric was calculated more frequently showed no significant differences. The total rest mass $M_{\rm rest} = \int dV D$ and angular momentum $J_{\rm rot} = \frac{1}{2}\int dV \rho h W^2 v_3$ are conserved to better than 10^{-3}.

Here we present the results from two representative models (Table 1). Note that the initial data slightly differ with respect to the value of β between the relativistic and Newtonian initial model. The time-evolution of the central density is plotted in Fig. 1. Model A is a strongly differentially rotating core which collapses rapidly ($t_{\rm bounce} = 38$ ms) due to the large reduction of $\gamma_{\rm p}$ from its initial value 4/3 to 1.30. The model bounces at a relatively high central density ($\rho_{\rm c}(t_{\rm bounce}) = 9.3 \times 10^{14}$ g cm^{-3}) because the supranuclear EoS was chosen to be extremely soft ($\gamma_{\rm p}(\rho > \rho_{\rm nuc}) = 5/3$). After bounce the rotating core oscillates with a superposition of various radial and axisymmetric modes. As expected, the oscillation frequencies of the core are higher in the relativistic model due to the higher densities achieved.

On the other hand, model B is initially an almost rigid rotator, which bounces later ($t_{\rm bounce} = 98$ ms) than model A due to its larger subnuclear adiabatic index $\gamma_{\rm p} = 1.325$. The collapse is stopped at subnuclear densities ($\rho_{\rm c}(t_{\rm bounce}) = 3.8 \times 10^{13}$ g cm^{-3}) by the rapid spin-up of the core due to angular momentum conservation. After bounce the core first expands, then begins to collapse once more and rebounces again. The phenomenon of homologous multiple bounces (which occurs with a period of roughly 40 ms (50 ms) in the relativistic (Newtonian) simulation; see lower panel in Fig. 1) was observed in the Newtonian simulations of Zwerger & Müller (1997) for strongly differentially rotating configurations with a sufficiently large initial value of β and a subnuclear $\gamma_{\rm p}$ close to 4/3. However, general relativistic models show distinct multiple bounces only for extremely rapidly and differentially rotating initial models. Most of the Newtonian models of Zwerger and Müller, which bounce at subnuclear densities, reach or even exceed in the relativistic simulations twice the maximum density of the Newtonian models. Thus, in many cases the central density largely exceeds nuclear matter density and the stiffening of the EoS destroys the coherence of the bounce.

The gravitational wave signature of both models is shown in Fig. 2, where we plot the quadrupole wave amplitude $A_{20}^{\rm E2}$ as defined in Zwerger & Müller (1997). For a source at a distance R the corresponding dimensionless strain is $h_{\theta\theta}^{\rm TT} = 8.85 \times 10^{-24} \sin^2\theta \cdot (A_{20}^{\rm E2}/1000) \cdot (10\ {\rm Mpc}/R)$, where θ is the angle between the line of sight and the rotation axis of the core.

For the rapidly collapsing model A with its soft supranuclear EoS the maximum central density of the relativistic simulation is almost 50% higher than in the Newtonian case. Nevertheless, the gravitational wave amplitude of the relativistic model is lower. This surprising result can be understood by noting that in the quadrupole formula the gravitational wave amplitude is determined by the second time derivative of the total quadrupole moment of the core, which involves a volume integral where the integrand is proportional to ρr^4. Thus a higher central density due to relativistic effects does not necessarily imply a stronger signal. Instead, one must take into account the entire density distribution. In Fig. 3 the profiles of ρ and ρr^4 at the equator ($\theta = \pi/2$) are plotted for the relativistic and the Newtonian model at $t_{\rm bounce}$. The density profile of the relativistic model is more compact than that of the Newtonian model, whereas the density of the latter model is larger for radii $\gtrsim 5$ km. This gives rise to its larger quadrupole moment (as the deformation of both models is comparable), and hence to its larger gravitational wave amplitude. (We note that Evans (1986) already observed the enhanced core compactness and breaking of homology in spherically symmetric relativistic collapse.)

In model B the relativistic effects cause the bounce to occur at much higher densities, and the interval between the multiple bounces is also shortened. In this case the gravitational wave amplitude of the relativistic model is actually somewhat larger than in the Newtonian one. As already pointed out, relativistic effects may play a key role in deciding whether a rapidly rotating core bounce will stall at subnuclear density (with a very distinctive gravitational waveform as in model B) or reach nuclear density (with a waveform as in model A). Therefore, such effects have to be taken into account when modeling rotational core collapse. We will investigate this issue further and present more quantitative results in an upcoming article.

As our relativistic simulations yield signal amplitudes similar to Newtonian models, the prospects for detection of rotational core collapse events are also similar. Therefore the predicted signal strength of Galactic events lies within the sensitivity range of the upcoming gravitational wave interferometers (Thorne 1997). However, extragalactic events seem to be too weak for current detector sensitivities. To further improve the waveforms, 3-dimensional effects and advanced microphysics have to be taken into account.

We appreciate contributions and suggestions from Y. Eriguchi, J. Mª Ibáñez, and G. Schäfer. The calculations were carried out at the Rechenzentrum Garching and MPI für Astrophysik, Garching.

REFERENCES

Alcubierre, M., Brügmann, B., Dramlitsch, T., Font, J. A., Papadopoulos, P., Seidel, E., Stergioulas, N., & Takahashi, R. 2000, Phys. Rev. D, 62, 044034
Banyuls, F., Font, J. A., Ibáñez, J. Mª, Martí, J. Mª, & Miralles, J. A. 1997, ApJ, 476, 221
Cook, G., Shapiro, S., & Teukolsky, S. 1996, Phys. Rev. D, 53, 5533
Eriguchi, Y., & Müller, E. 1984, A&A, 147, 161
Evans, C. R. 1986, in Dynamical spacetimes and numerical relativity, ed. Centrella, J., 3 (Cambridge: Cambridge University Press)
Font, J. A. 2000, Living Reviews in Relativity, 3 http://www.livingreviews.org/Articles/Volume3/2000-2font/
Heger, A., Langer, N., & Woosley, S. E. 2000, ApJ, 528, 368
Janka, H.-T., Zwerger, T., & Mönchmeyer, R. 1993, A&A, 268, 360
Kley, W., & Schäfer, G. 1999, Phys. Rev. D, 60, 027501
Komatsu, H., Eriguchi, Y., & Hachisu, I. 1989, MNRAS, 237, 355
May, M., & White, R. 1966, Phys. Rev., 141, 1232
Mönchmeyer, R., Schäfer, G., Müller, E., & Kates, R. 1991, A&A, 246, 417
Müller, E. 1998, in Computational methods for astrophysical fluid flow, Saas-Fee Advanced Course 27, ed. Steiner, O., & Gautschy, A., 343 (Berlin: Springer)
Rampp, M., Müller, E., & Ruffert, M. 1998, A&A, 332, 969
Thorne, K. 1997, Rev. Mod. Astron., 10, 1
Wilson, J. R., Mathews, G. J., & Marronetti, P. 1996, Phys. Rev. D, 54, 1317
Flanagan, É. É. 1999, Phys. Rev. Lett., 82, 1354
Mathews, G. J., & Wilson, J. R. 2000, Phys. Rev. D, 61, 127304
Zwerger, T., & Müller, E. 1997, A&A, 320, 209

TABLE 1
MODEL PARAMETERS

Model	A [10^8 cm]	$\beta_{\rm R}$ [%]	$\beta_{\rm N}$ [%]	$\gamma_{\rm p}$ ($\rho \leq \rho_{\rm nuc}$)	$\gamma_{\rm p}$ ($\rho > \rho_{\rm nuc}$)
A	0.5	0.47	0.48	1.300	5/3
B	1.0	1.82	1.81	1.325	—[a]

[a] Note that model B never reaches supranuclear densities.

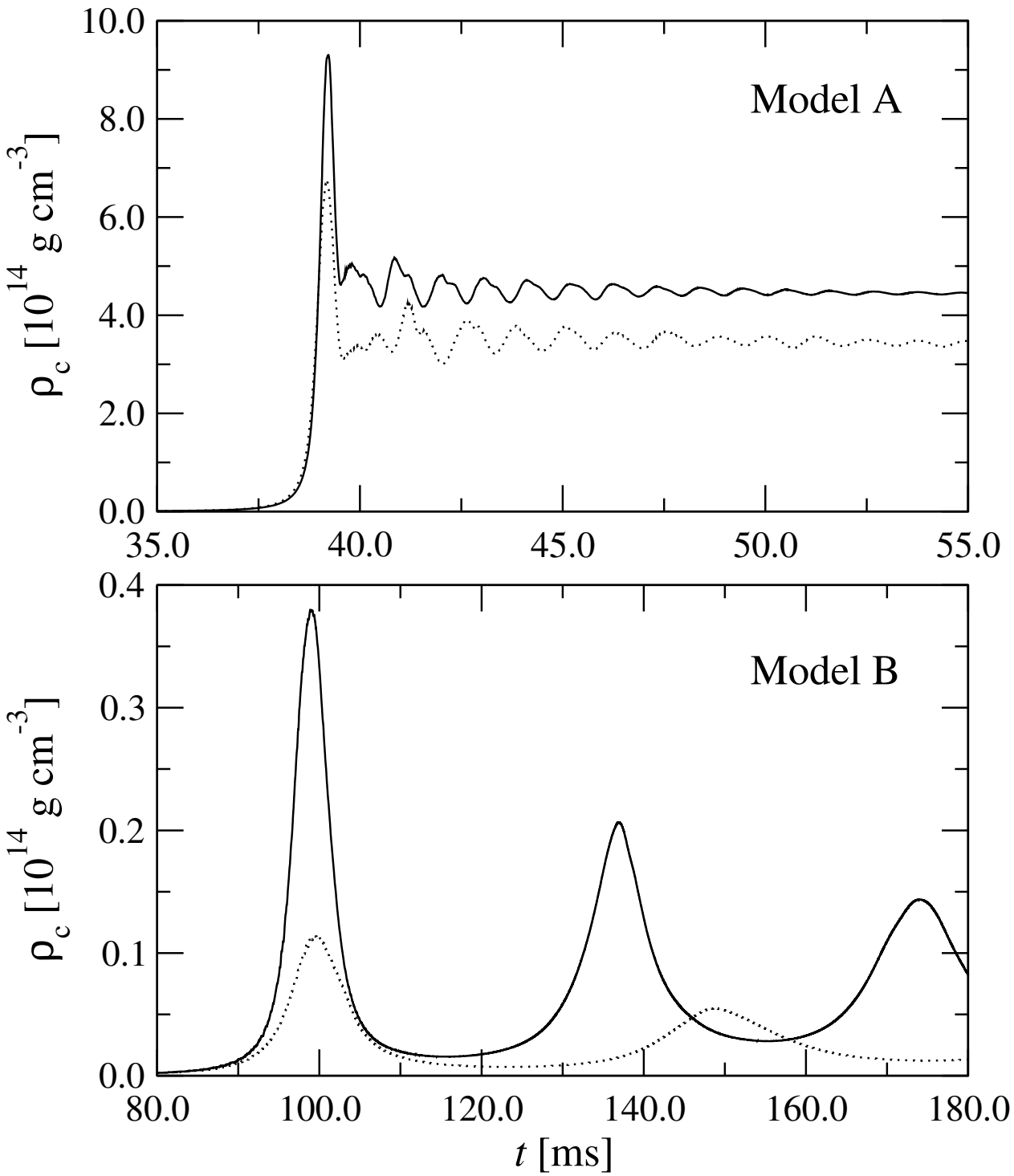

FIG. 1.— Central density vs. time for model A (upper panel) and B (lower panel); relativistic runs are denoted by solid lines, Newtonian runs by dotted lines.

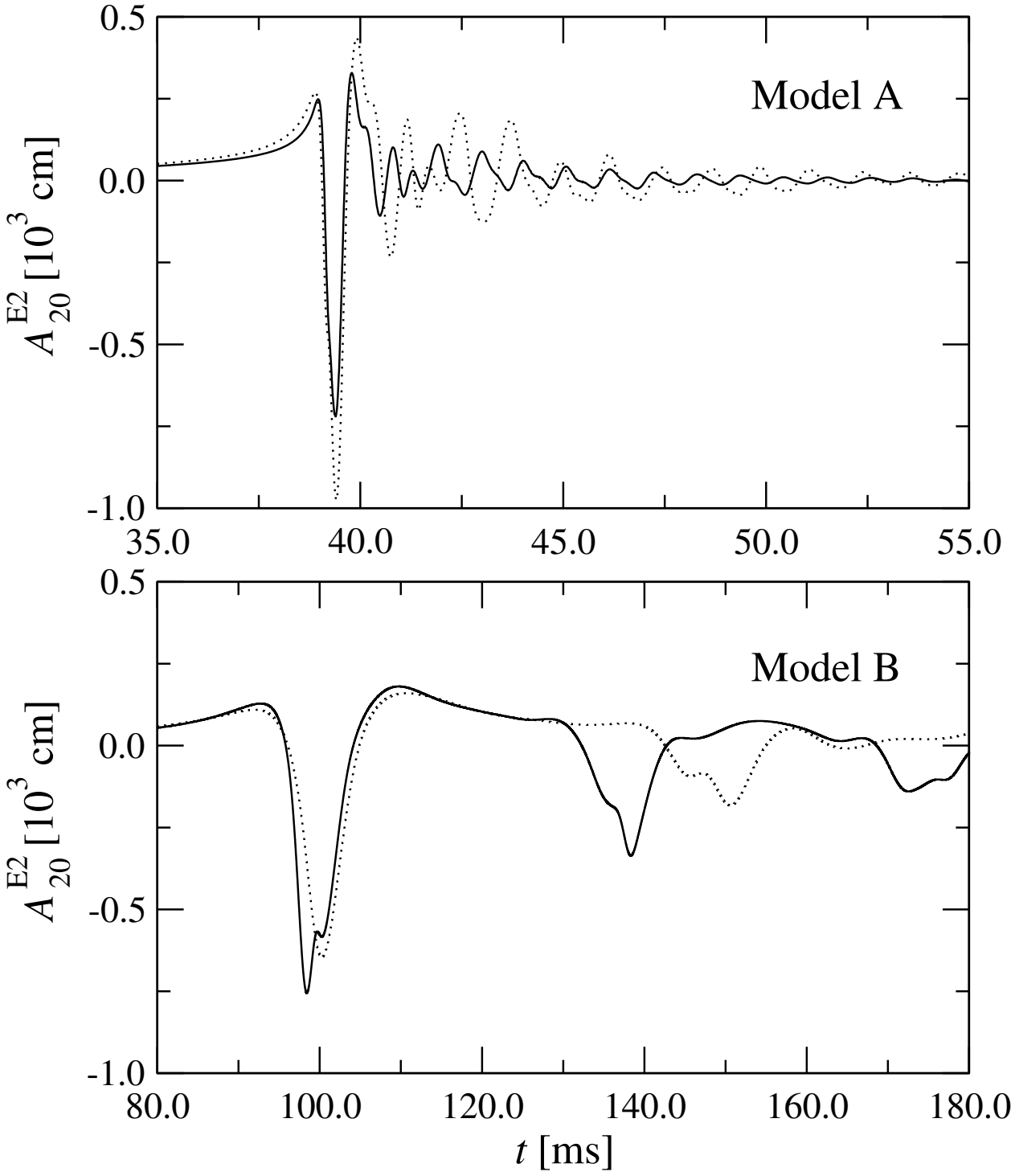

FIG. 2.— Quadrupole gravitational wave amplitude for model A (upper panel) and B (lower panel); relativistic runs are denoted by solid lines, Newtonian runs by dotted lines.

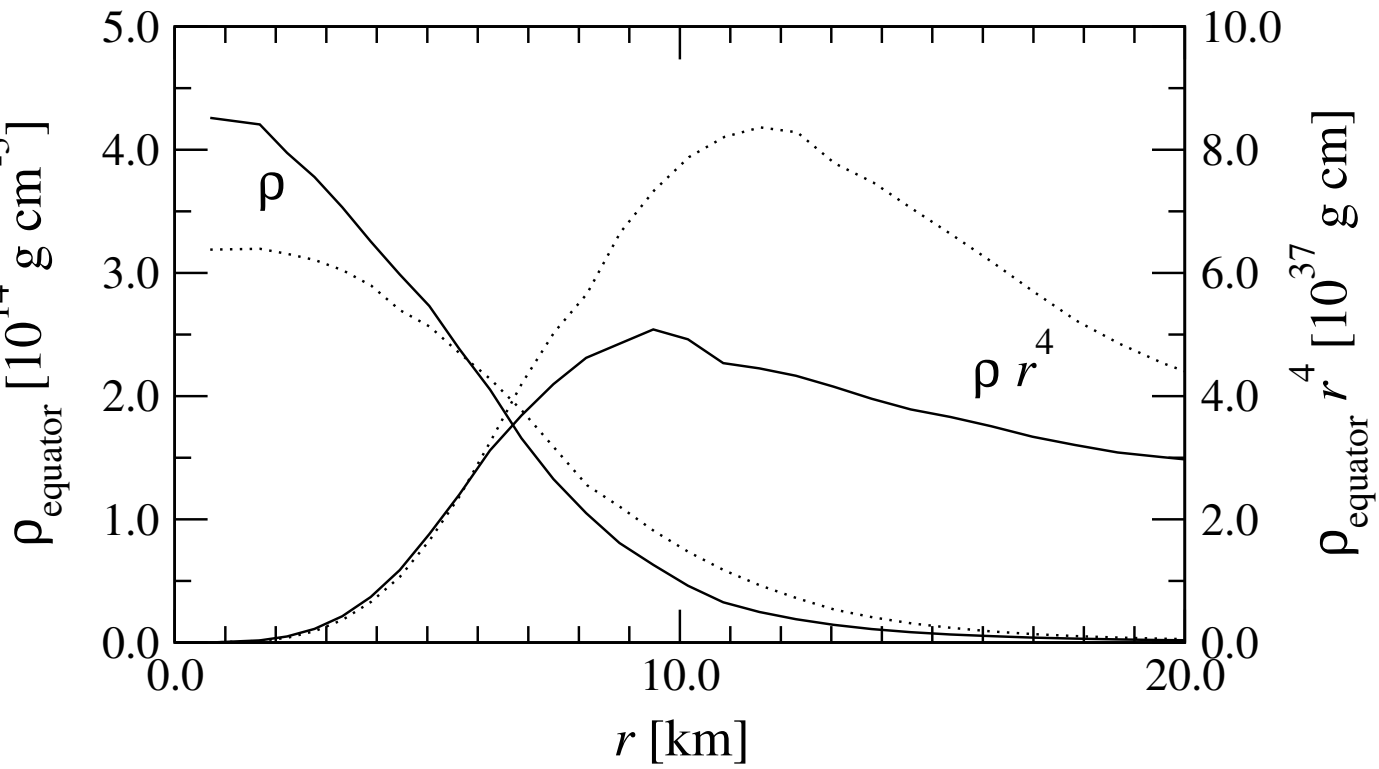

FIG. 3.— Equatorial profiles of the density ρ and ρr^4 of model A at bounce obtained in a Newtonian (dotted lines) and relativistic (solid lines) simulation.